13

Computational Neuroimaging: Color tuning in two human cortical areas measured using fMRI

Brian A. Wandell, Heidi Baseler, Allen B. Poirson, Geoffrey M. Boynton and Stephen Engel

Introduction

The neural representation of the visual world begins with the responses of four interleaved photoreceptor mosaics. These photoreceptor mosaics simultaneously encode information about pattern, motion and many other aspects of the visual world. As early as the photoreceptors themselves, neural specializations exist that distinguish among the many kinds of information contained in the photoreceptor mosaics. For example, the photoreceptors are divided into rods and cones, specialized for different types of viewing conditions. At the next synapse, foveal cones are each contacted by bipolar cells with many different morphologies, interconnection patterns, and receptive field properties. These different types of cells appear to segregate information into streams that are specialized for different tasks.

The diversity of neural form and function observed within the retina is present thoughout the visual pathways. What is the relationship between this diversity and our perceptual experience of the world?

Theories of vision are dominated by the hypothesis that there is a direct correlation between the segregation of function at the neural level and the segregation of *perceptual attributes*. Namely, every day we make perceptual judgements that separate color from shape, motion and other stimulus attributes. Most recent theories suppose that the cell diversity and perceptual experience can be related in a straightforward fashion.

For example, Zeki et al. have argued that in the monkey brain neurons within area V4 are specialized for representing color information (Zeki et al., 1991). This view has been challenged by Cowey and Heywood, who accept the basic conceptual framework, but proposes area TEO instead (1995). Hubel and Livingstone (1987) have also argued in favor of the general hypothesis of functional segregation and proposed that the origins of neural specialization of color can be traced to the responses of neurons within specialized regions of V1 and V2. Retinal anatomists have suggested that the segregation of perceptual color information can be identified in the retina (e.g., Rodieck, 1991), and this view has obtained further support from Dacey and Lee's (1994) observations concerning the specialization for S cone signals carried by the small bistratified retinal ganglion cells.

In human cortex, two main types of evidence are used to support the hypothesis of a functional segregation and specialization for color appearance. Meadows (1974) analyzed a number of cases of brain damage in which several subjects' perception of color was disturbed, but acuity, motion and other visual functions were not. This syndrome, which I will call cerebral dyschromatopsia, was reviewed thoroughly by Zeki (1990). While dyschromatopsia is accompanied often by several visual deficits, such as face blindness (prosopagnosia) and upper visual field loss, these associations are not always observed. Because there are some patients with color loss and no discernible prosopagnosia, and other patients with prosopag-

nosia but no discernible color loss (a double dissociation), Meadows, Zeki and many others have accepted the view that color has a discrete representation in the cortex.

Neuroimaging studies provide a second source of evidence for functional specialization of the color representation in the human brain (Lueck et al., 1989; Zeki et al., 1991). These authors compared the size of the PET signal when subjects viewed a collection of full-color rectangular patches compared to monochrome images consisting of the same rectangles matched in luminance. The difference signal is particularly large in a region of the brain ventral to calcarine cortex, near the upper field representation of primary and secondary visual cortical areas. Zeki and his colleagues take this observation to support the hypothesis that color processing is functionally specialized and segregated in human cortex. The measurements themselves have been partially confirmed by Sakai et al. (1995), though other measurements by Gulyas et al. (1994) and Engel, Zhang and Wandell (1997) suggest a different organization.

Neither the lesion data nor the neuroimaging data are conclusive. First, consider the case of cerebral dyschromatopsia. We might try to understand the implications for cerebral loss in this condition by comparing it with a fairly well understood color deficit: the loss of color vision caused by an inherited color deficiency resulting in the absence of at least one type of cone (dichromacy). The color confusions of dichromats are quite significant, though there is little or no loss of visual acuity or motion selectivity. Yet, we do not argue that color vision is functionally segregated and specialized in the photopigments. Nor do we argue that other types of information, such as motion and form, are not carried in the photoreceptors.

At the level of the photoreceptors, we already understand that color appearance reflects the coordinated action of a system of neurons and disruption of one type of photorceptor leads to color anomalies; but no photoreceptor class is the unique site of color vision. We also understand that motion information is carried in the space time response of the photoreceptors, so that disruption of one photoreceptor class will not eliminate information needed to perform most motion discriminations or estimations. Beyond the receptors, functional specialization for perceptual attributes is a poor description of retinal pathways. Trichromacy is determined by the cone properties, but the cones are used for much more than color. The specialized rod pathway, via the AII amacrines, is important for rod vision, but the rod signals merge onto a cone pathway after only a few synaptic connections. There are few grounds to argue that retinal specializations are equated with perceptual experiences.[1]

The neuroimaging data, based on the subtraction methodology, are not decisive either. The experimental data reveal several cortical regions where activity is greater to the full-color color image rather than the monochrome image. Necessarily, there will be one region with the largest difference; it could not be other. As used by Zeki the subtraction methodology (described by Posner & Raichle, 1994) identifies color appearance with this single region. But the existence of a largest response does not imply that other differences should be ignored, nor that color is localized rather than part of a distributed representation. Indeed, authors who favor distributed representations theoretically, use neuroimaging data to emphasize the distributed nature of neural responses during color, motion and stereo tasks (e.g., Gulyas et al., 1994).

Finally, let us return to the perceptual basis for the functional segregation hypothesis: some perceptual attributes, such as color can be separated from other perceptual attributes, such as motion, depth, and form. As an empirical observation, this claim is only roughly true. The apparent velocity of an object varies depending on the object's contrast and color (Cavanagh & Anstis, 1991; Gegenfurtner & Hawken, 1998); the color of a pattern depends on its spatiotemporal properties: high spatial and temporal frequency patterns appear light-dark, and very desaturated (Poirson & Wandell, 1993). It is difficult to find conditions in which we do not know both the location and the color, so that one might argue that color and spatial position

1. Though such specializations have been claimed (Lettvin et al., 1959).

(and motion and pattern) are tightly coupled, not dissociated. Hence, it is possible to use the perceptual literature to argue that there is a close coupling of color and other visual information, not a complete segregation.

We began this section with the claim that the arguments in favor of functional specialization are not conclusive. It is also true that the criticisms of the hypothesis presented here do not falsify it. Rather, the criticisms show that the evidence in favor of functional specialization and segregation is weak, and that it is a good moment to formulate alternatives and seek further empirical tests. To begin this process, we find it useful to consider the retina as a model system because we know much about the organization of information in the retina compared to the brain. What do the principles of information representation in the retina suggest that we might find in seeking to uncover the representation of information within cortex?

Computational Neuroimaging. We are studying the hypothesis that the neural diversity observed using anatomical and electrophysiological methods represents a computational diversity, rather than functional specializations associated with perceptual attributes. Guided by this hypothesis, we are developing methods we call *computational neuroimaging* in order to measure the neural computations applied to stimulus information. Our experiments are designed to answer questions about the nature of the computation performed along specialized pathways: how do neurons within cortex transform visual information?

This approach flows from our current understanding of retinal processing. Within the retina, information about pattern, movement and color often flow together in common pathways. The pathways themselves -- such as the different types of horizontal cell pathways or the different ganglion cell pathways -- appear to be specialized for certain kinds of computations. The HI and HII type horizontal cell mosaics perform separate computations that appear to regulate the gain of signals originating in different parts of the spectrum (Dacey et al., 1996). The midget and parasol cells appear specialized for encoding information about different spatiotemporal components of the image (Wandell, 1995).

If cortical diversity is also based on the need to perform different types of specialized computation, we would not ask: Where is color located? Rather, we would ask: How do neurons transform and relay the signals sent to them, and how do these transformations achieve the computational goals related to color (or motion, or depth) perception?

Adopting this computational view, we might also interpret lesion data differently. Rather than interpreting the lesion data as the destruction of a perceptual representation, we would view the lesions as a disruption of an information processing task that is essential for color computations. Interference with certain types of processing routines may have serious consequences for color vision and perhaps other functions. We would not conclude that the lesion sites are also the locus of a unique color representation, any more than the wavelength transduction computed by the photopigment absorptions is the site of color vision.

To develop an empirical basis for this conceptual framework, we have been using functional magnetic resonance imaging to measure how color information is distributed and transformed within human cortex. Our intial measurements of color cortical tuning in areas V1 and V2 were described in Engel, Zhang and Wandell (1997); here we report on additional observations of color tuning in extrastriate cortex located near the lingual and fusiform gyri. These measurements form part of a general project of measuring color responsivity across visual cortex under a variety of stimulus conditions. In this way, we hope to understand the distribution of color information and to detect locations where computations specialized for color computations may reside within cortex.

Methods

Because functional magnetic resonance imaging (fMRI) is a relatively new method for analyzing human cortical activity, we begin with some background on the method and our view on how it might be used to trace the distribution of cortical color informa-

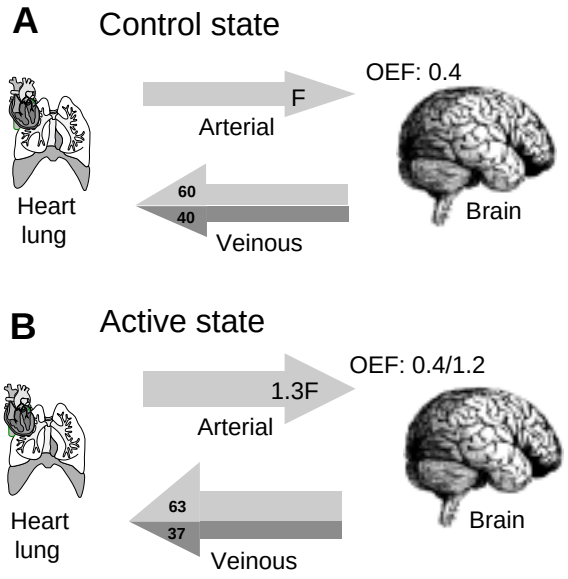

Figure 13.1: Activity-dependent changes in blood-oxygenation. (A) In the control state, the arterial supply is fully oxygenated and forty percent of the oxygen is used. (B) In an activated state, there is an increase in the total volume of blood oxygen delivered to the active region. The local oxygen consumption increases, but the oxygen supply exceeds the needs resulting in a relative increase in veinous blood oxygen.

tion. Then, we describe the specific methods we used in the experiments reported here.

The fMRI signal: background. The magnetic resonance signal measures the rate at which dipoles, present within a uniform magnetic field, return to the equilibrium after being perturbed by a radio frequency (RF) pulse. The two rate parameters associated with the return of the dipole vector to equilibrium can be measured separately; these two rate parameters, T_1 and T_2, are influenced by different aspects of the local magnetic field. The physical significance of these rates parameters can be understood as follows. Suppose we begin with a vector oriented in the vertical direction. When we rotate the vector off axis, the vector difference between the initial position and the rotated position has a horizontal and a vertical component. The time constants describe the exponential relaxation back to equilibrium of the vertical (T_1) and horizontal (T_2) components.

In the case of the functional magnetic resonance imaging, the signal governed by the second rate parameter, T_2 is measured. The fMRI signal depends on the observation that oxygenated (HbO2) and de-oxygenated (Hb) blood have different magnetic field properties (Thulborn et al., 1982). Oxygenated blood (HbO) is magnetically transparent (diamagnetic) while de-oxygenated blood (Hb) is not (paramagnetic). After being perturbed by an RF pulse, dipoles near Hb return to their equilibrium state more rapidly than dipoles near HbO.

Fox and others (Fox & Raichle, 1986; Fox et al., 1988) showed that changes in neural activity cause a 30-50 percent increase in cerebral blood flow near active cortical regions (activity may be due to excitation or inhibition, or any metabolic process), but only a 5 percent increase in oxygen metabolic rate. The situation is illustrated in Fig. 13.1. In a control condition, arteries supply nearly 100 percent oxygenated blood and roughly 40 percent of the oxygen is consumed locally, so that the blood returning in the veins comprises 60 percent oxygenated and 40 percent deoxygenated blood. During a stimulus condition that causes significant neural activity, an additional supply of oxygenated blood is delivered, but only a small fraction of this supply is metabolized. Hence, the fraction of extracted oxygen is smaller compared to the control state, and the proportion of oxygenated and deoxygenated blood becomes 63:37. The change in the ratio of oxygenated and deoxygenated blood changes the rate at which the dipoles return to steady state following an RF pulse. By comparing the rate of return one can make an inference about the local neural activity. This signal is called the blood oxygen level dependent (**BOLD**).[2]

The flow of information illustrated in Fig. 13.2 helps to remind us of the complexity of the signalling path in an fMRI experiment. The choice of signal and control stimuli result in two patterns of neural activity; the neural differences result in oxygenation differences. The relationship between the MR signal (output) and the stimulus level (input) is not well

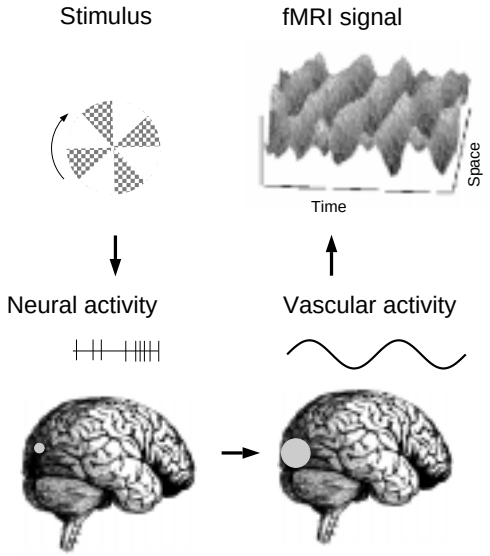

Figure 13.2: The fMRI imaging pathway. The stimulus causes neural activity. The neural activity changes the spatial distribution of blood oxygen. The blood oxygen distribution influences the local magnetic field, resulting in a spatial variation in the MR signal.

understood and depends on both of these intermediate steps (signal to neural activity, neural activity to oxygenation level), both of which may be nonlinear.

The display system was calibrated in situ, using light scattered from the final mirror, using a PhotoResearch spectral radiometer and a hand-held Minolta photometer. We measured the spectral power distribution of each of the color channels at maximum intensity using a PhotoResearch spectroradiometer. We measured the gamma curve of the system (framebuffer to display intensity) for each of the channels and verified the independence of the three color channels outputs (cf. Brainard, 1989). Because of constraints on placing equipment in the scanner room, and inhomogeneities in the display equipment, these measurements are accurate to a factor of about 10 percent.

Stimuli were circular, 20˚, contrast-reversing, circular, checkerboard patterns presented on a larger neutral mean field luminance, Y, of 72 cd/m^2 and an xy chromaticity of [.30, .40]. We describe the stimuli using contrast levels based on the Smith-Pokorny cone fundamentals. Specifically, suppose the values L_0, M_0, and S_0 represent the long, medium and short wavelength cone absorptions from the mean field, and ΔL, ΔM, and ΔS, represent deviations from this mean value introduced by a specific color of the checkerboard pattern. Then, we describe the checkerboard contrast by the vector $s = (\Delta L/L_0, \Delta M/M_0, \Delta S/S_0)$. The *color direction* of the stimulus is the unit length vector $s/||s||$.

The stimulus sequence. A spatial image of a black-white version of the checkerboard pattern, at a single moment in time, is shown in Fig. 13.3A. The contrast pattern consisted of a balanced set of positive and negative modulations about the mean field. The stimulus consisted of a fine pattern near its center that became increasingly coarse with eccentricity. Subjects fixated at the center of the target throughout the scan. For the data described here, the checkerboard contrast-reversed at 1 Hz.

During the MR scans, the contrast-reversing stimuli were presented as part of a stimulus-control pair. A contrast-reversing pattern (see Fig. 13.3) was presented for 15 s, followed by 27 s control consisting of a uniform field at the mean illumination level. In this way, the response to the signal could always be compared with the control level presented in an adjacent time period.

Stimulus-control pairs were presented in triplets (see Fig. 13.3B). The three stimuli in a triplet shared a common color direction, but the stimulus contrast increased (or decreased), consecutive stimuli changing in contrast by a factor of two. Hence, a single triplet might consist of an (L,M,S) contrast series such as (.1,.1,0), (.2,.2,0), (.4,.4,0).

2. Fox and co-workers suggested that the large increase in blood flow compared to metabolized oxygen was a mis-match between two decoupled mechanisms. Buxton and Frank (1997) suggest that the difference is to be expected if we accept that (a) under rest conditions capillaries are perfused and (b) extracted oxygen is fully metabolized. Whether the two mechanisms are decoupled, or intimately linked, will be important for interpreting the neural significance of the fMRI signal.

Six stimulus-control patterns were presented during each fMRI scan, representing two randomly chosen color directions within the (L,M) color plane (i.e., S=0). Six fMRI scans were performed during a single experimental session. Hence, during a single session responses were measured to stimuli in six color directions, each consisting of three contrast levels. During each session every stimulus-control pair was presented twice, once as part of an increasing sequence and once as part of a decreasing sequence, for a total of thirty-six stimulus-control presentations.

Response Amplitude. We measured the amplitude of the fMRI signal within a region of interest (ROI) using the following sequence of operations.

1. The ROIs were selected in two steps. First, two coarse ROIs were selected based on anatomical criteria. The first spanned area V1 as determined in separate studies of the retinotopic organization (Engel, Zhang & Wandell, 1997). The second spanned a large region of ventral occipital cortex and was selected to be distinct from the retinotopically mapped areas identified ine arlier studies.

2. Second, the ROIs were refined by fMRI activity. Pixels in the coarse ROI were retained only if their response at the stimulus frequency rose to 30 percent of the signal variance for at least one of the color stimulus conditions. The reason for applying this second step is this: voxels (1.5 x 1.5 x 5 mm) measured during the functional scans often include a mixture of gray matter and other unwanted substances, an effect called *partial voluming*. It is difficult to identify which voxels contain primarily gray matter, and which do not. By restricting the ROI to responsive voxels, we reduce the noise introduced by partial voluming.

3. We measured the response using the average timeseries of the voxels in each ROI. First, we divided the timeseries into the 42 s stimulus-control periods and calculated the amplitude of the fMRI signal harmonic at the one period per 42 s (1/42 Hz). Second, we estimated the noise during a scan by calculating the amplitudes at temporal frequencies other frequencies. Based on earlier measurements of noise, we have determined that the noise power spectrum is well fit a decreasing exponential function. Hence, we fit this function to the scan measurements and used the interpolated amplitude at 1/42 s Hz as the noise amplitude estimate. Finally, we removed the estimated noise from the amplitude of the fMRI signal at the signal frequency, using the method described in the Appendix. We call the amplitude following removal of the noise the *response amplitude* and this value, measured in percent modulation, is reported in our graphs.

Results

In a brief separate report, we described measurements of color tuning in areas V1 and V2 for contrast-reversing patterns at 1, 4 and 10 Hz. The color responses were strongest per unit cone contrast for signals in the L-M (i.e., red-green) opponent (Engel, Zhang & Wandell, 1997; see also Kleinschmidt et al., 1996). These measurements parallel, in some regards, the visual sensitivity to these same stimuli.

Here, we report color responses we have measured in other positions within extrastriate cortex. The next few paragraphs and figures describe some of this activity and color tuning measurements from activity near the lingual and fusiform gyri of two observers.

The ventral occipital ROI (VO-ROI) spanned several imaging planes for both subjects. These planes are located roughly 2 cm anterior of the posterior pole, and spaced by 8 mm. Fig. 13.4 shows the location of VO-ROI in several planes located perpendicular to the calcarine. The locations of the measurement planes can be the seen in the anatomical localizer shown at the left of the figure.

Fig. 13.5 shows the spatial distribution of activity during one typical functional scan. The locations of brain regions with a correlation level of at least 0.3 are shown. The methods used to calculate the correlations are described in detail in Engel, Zhang and Wandell (1997). The stimulus caused significant activity outside of areas V1 and V2. The planes shown in Fig. 13.5 were chosen because they each contained significant activity in regions near the fusiform and lingual gyri, which have been correlated with prosopagnosia and achromatopsia (Meadows, 1974; Zeki et al., 1991).

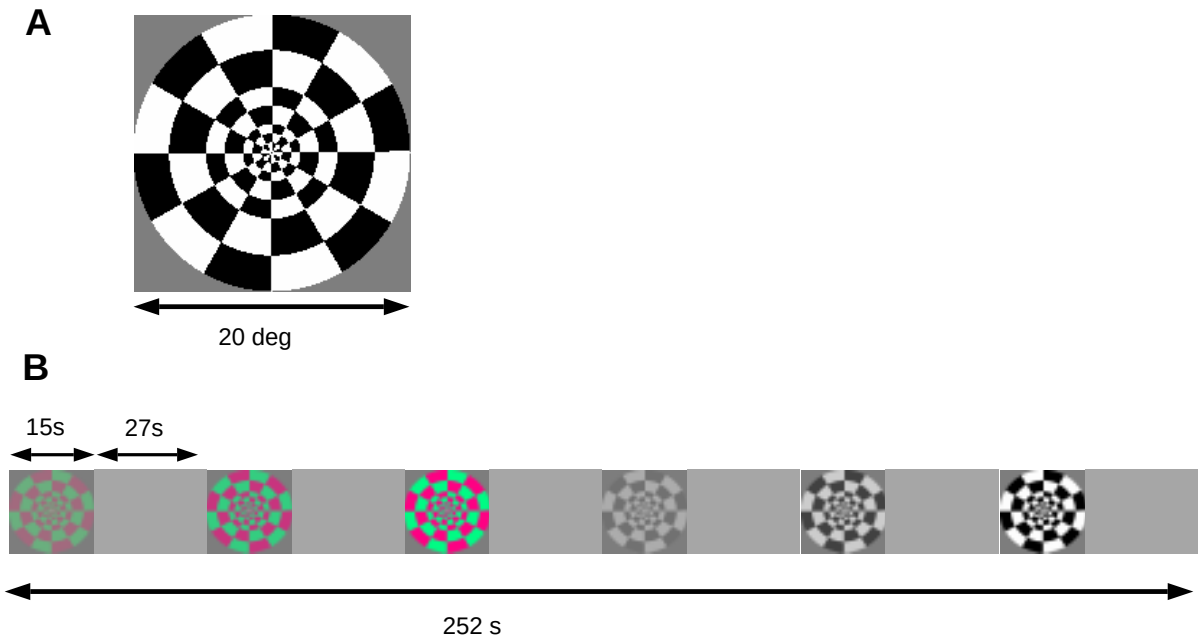

Figure 13.3: The stimulus and an example stimulus sequence shown during a single scan. (A) The spatial structure of a black-white version of the stimulus, at a single moment in time, is shown. (B) During each 252 s scan, six stimulus-control combinations were presented. The first three stimuli shared a common color (red-green in this example) but varied monotonically in contrast. The next group of three stimuli shared a common color (white-black in this example) that differed from the first three. In half of the scans the stimulus contrast increased by a factor of two between stimuli, as shown here. In the remaining scans the stimulus contrast decreased by a factor of two between stimuli.

Naturally, we were interested to consider whether the color tuning in these areas differed significantly from the tuning reported in areas V1 and V2 (Engel, Zhang & Wandell, 1997).

Fig. 13.6 shows the fMRI timeseries measured in the two regions of interest during presentation of 12 different colored targets. Panels (A) and (B) show the fMRI signals as subject BW viewed four different colored flickering patterns, each shown at three (increasing) contrast levels. Panels (C,D) show replications of this experiment for subject SE. The solid curves show the signals within area V1, and the dashed curves show the signals within the ventral occipital lobe.

The fMRI signal followed the onset and offset of the flickering pattern; and, the amplitude of the signal followed the contrast of the signal. For subject BW, the amplitude of the signals within area V1 and in the ventral occipital region were roughly equal; for subject SE the amplitude in the ventral occipital region was approximately 1.5 times greater than the amplitude in the V1 region.

The relative amplitudes measured in the two regions differed somewhat, but there was close agreement between the amplitudes of the signals measured within V1-ROI and VO-ROI. The response amplitudes in the two regions are compared in Fig. 13.7. The horizontal axis measures the amplitude of the response amplitude measured in the V1-ROI and the vertical axis measures the amplitude in VO-ROI. The two panels show the results for the two observers. For BW the response amplitudes in V1-ROI and VO-ROI are of similar magnitude; for SE the ventral occipital response is roughly 1.5 times the response within area V1. The response amplitudes correlate at 0.82 and

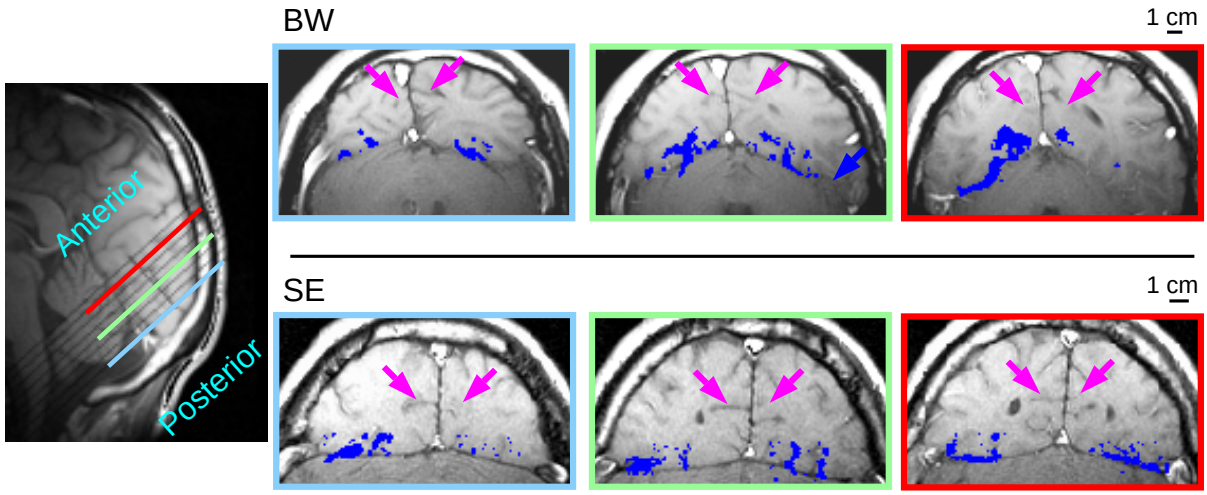

Figure 13.4: The location of the ventral occipital ROI (VO-ROI). The image planes were chosen perpendicular to the calcarine cortex. The positions of the planes are indicated by the colored lines on the sagittal image of subject SE on the left; image planes for BW were similar. The corresponding images for both subjects are shown on the right, with a bounding box in a color that matches the line shown on the left. The location of the VO-ROI within each plane is denoted by the blue overlay. The location of the calcarine sulcus is indicated by the magenta arrows. Area V1 is located several cm away from the VO-ROI, as measured along the surface of cortex. The centimeter scale bar is slightly different for the two subjects, but consistent across the separate images for each subject.

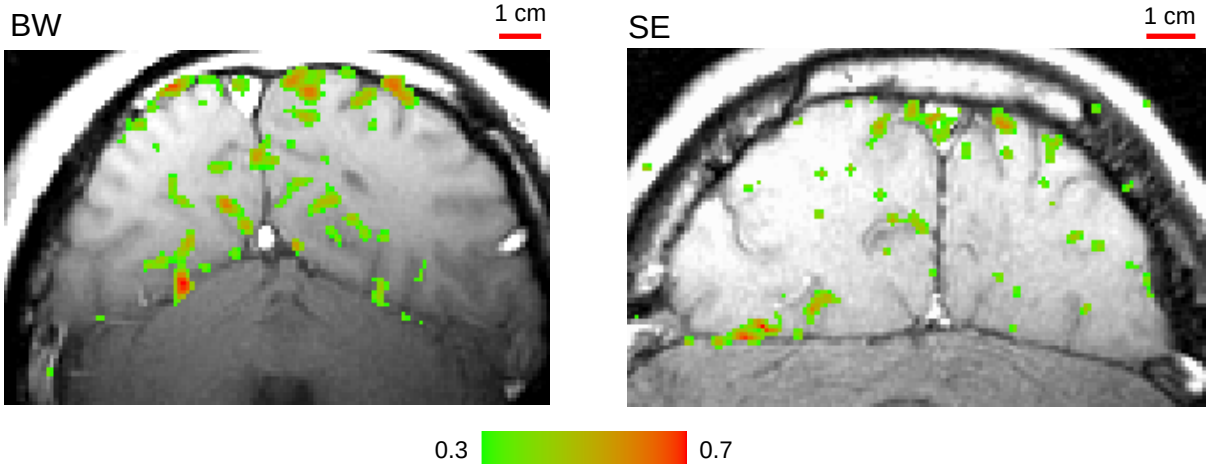

Figure 13.5: Spatial distribution of the active locations for a typical stimulus sequence. The image planes show activity in the planes denoted as green (left image, BW) and blue (right image, SE) planes shown in Fig. 13.4. The color bar at the bottom indicates the correlation level. Only locations with correlation exceeding 0.3 are shown.

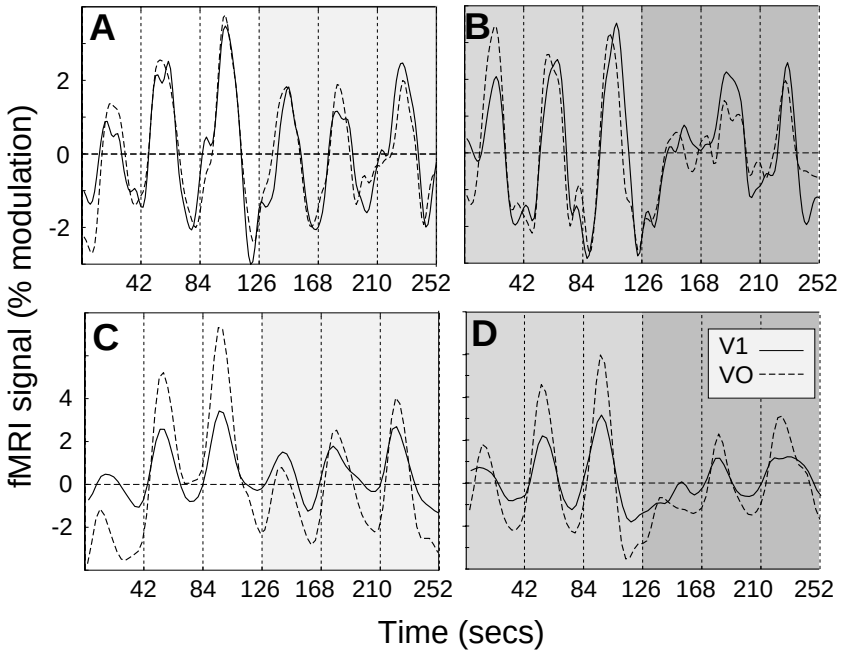

Figure 13.6: Timeseries of the fMRI signal within the V1 region of interest (V1-ROI) (solid lines) and the VO-ROI (dashed lines) are shown. (A,B) The fMRI signal during two separate experimental sessions, each lasting about 4 minutes, is shown. Within each session, the observer viewed six separate targets that varied in color and contrast; the shading indicates targets with the same color, differing only by contrast. (C,D) These are data for subject SE; the conditions and plotting conventions are the same.

0.89 levels suggesting that there is a common signalling path between these regions.

One puzzling aspect of the signals is the vertical offset: at low V1 signal levels, there is still a measurable signal in VO-ROI. We do not know if this is due to reduced noise levels in the VO-ROI region compared to V1-ROI, or whether the data represent a genuine difference in the brain activity.

A second method of comparing the responses in these two areas is by examining the iso-response curves to different colored stimuli. Fig. 13.8 shows the iso-response curves in V1-ROI (A,B) and VO-ROI (C,D). Consistent with our previous report, the strongest response per unit cone contrast is in an opponent-color direction (1,-1,0) (see Engel, Zhang & Wandell, 1997). The color iso-response curves for subject SE are nearly identical in the two regions. The iso-response curves for BW are not precisely the same. Because of the uncertainty in the measurements (indicated by the large confidence interval) we cannot reject the hypothesis that the two data sets share a common color tuning function under these measurement conditions. Methods for computing the confidence intervals are explained in the appendix.

At these low spatio-temporal frequencies, and in the (L,M) color plane, we are observing two copies of the same color signal. We plan to extend these test conditions using test and adapting stimuli that (a) strongly stimulate the S-cones, (b) have a variety of spatiotemporal properties, (c) a vary the adapting conditions. The systematic measurements of the large signals within these areas will allow us to determine whether across all conditions the signal is copied, or whether certain aspects of the signal represented in V1 are transformed as the neural responses spread into other regions of the brain.

Related Work

Neuroimaging work. There have been roughly a dozen papers using functional neuroimaging methods to measure human cortical color representation. One set of papers, including both those based on positron emission tomography (PET) and fMRI, use the subtraction methodology (Posner & Raichle, 1994) to identify a color center of the brain, an enterprise that is widely called *brain mapping*.

The studies by Zeki et al. (1991) and Sakai et al. (1995) set out to identify a focal area associated with color perception. Both groups used the subtraction methodology and compared the activity levels elicited by a pair of related. In both cases, one stimulus was a simple colored pattern and the comparison stimulus had the same shape and timecourse, but was an achromatic pattern. The achromatic pattern was matched in luminance (but not chromaticity) to the colored pattern. Both groups report that in comparing the difference between these two patterns, a high degree of statistical significance was observed near the VO-ROI in the lingual and fusiform gyri. Neither group reports the absolute size of the responses elicited by the individual stimuli, but they do report that the individual stimuli did generate considerable activity in calcarine sulcus.

Zeki et al. (1991) do not specify the color coordinates of their stimuli. Sakai et al. (1995) specify the color coordinates of the colored stimulus, but not of the matched achromatic stimuli. Our calculations, based on the assumption that achromatic patterns refer to a standard white, suggest that the largest contrast difference between the colored and achromatic stimuli is seen by the short wavelength cone receptors. Hence, it is possible that the reason for the reported difference in activity between the colored and achromatic Mondrians is due to differential signalling by a pathway specialized for carrying S-cone signals, a possibility we have not examined in this paper.

Gulyas and Roland (1994) report using colored stimuli as part of their investigations of cortical processing. Gulyas and Roland set out to understand the distribution of activity throughout the brain as subjects engaged in tasks that involved color discrimination, form discrimination, and depth judgments. The use of color was only incidental to their main objective: to understand how different types of task evoke activity in different brain networks. For all of experimental tasks, they report significant activity in a broad array of brain locations. The stastically significant regions activated during colour detection were more numerous and widespread than those in form detection.

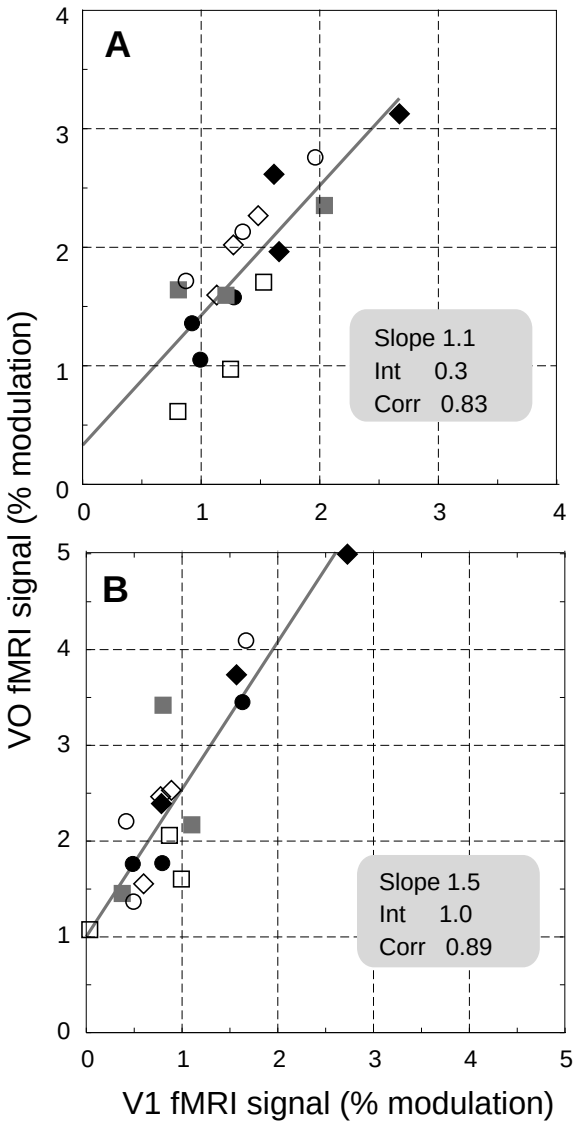

Figure 13.7: Response amplitudes in V1-ROI (horizontal axis) and VO-ROI (vertical axis) are compared. Different symbols refer to measurements with different colors; there are three symbols of each type corresponding to the three contrast levels of each color. Panels (A) and (B) are for subjects BW and SE, respectively.

Kleinschmidt et al. (1995) and Engel, Zhang and Wandell (1997) measured the fMRI signal obtained by alternating a colored contrast pattern and a neutral, uniform field. Kleinschmidt et al. (1996) compared the

response to several colored stimuli, including L-M, S, and L+M stimuli. Engel, Zhang and Wandell made similar measurements, but they (a) concentrated in retinotopically areas V1 and V2, and (b) measured color tuning using a larger variety of color stimuli, and (c) compared the fMRI color tuning with behavior. Fig. 13.1C in the Kleinschmidt et al. paper and Fig. 13.5 here agree well, despite differences in MR methods and display instrumentation. Both groups report activity in calcarine cortex and in ventral occipital lobe. Both groups report that, per unit cone contrast, the L-M direction produced a larger fMRI response. Here we confirm Kleinschmidt's observation that there is also significant signal in the ventral occipital lobe. We add the observation that the color tuning in this region is quite similar to the color tuning we have reported in area V1.

The approach taken by Kleinschmidt et al. and our group is based on establishing the nature of the color signal at different points in cortex, rather than locating a single color center. Hence, the first set of questions posed by both groups are structured in terms of how signals initiated within the retina are distributed within cortex. Subsequent experiments will address how these signals vary with spatial, temporal, and other properties of the input signal. Ultimately, we hope to understand how the set of transformations within cortex explain our perceptions of color.

Single-unit work. The most detailed information we have about color information in cortex comes from studies of single-unit recordings in monkey models. Because of the great technical challenges in making these measurements, there have been few attempts to make complete measurements of the spatio-temporal-chromatic response functions of individual units. Instead, the majority of the single-unit literature parallels the neuroimaging literature. Most authors seek partial characterizations, often with the goal of labeling a neuron to classify it as color selective or not.

The papers containing the most complete characterizations to date are those from Lennie, Gegenfurtner and their collaborators. In these studies, efficiency dictated that only a limited portion of the neuron's responsiveness be measured. For example, Lennie, Krauskopf and Sclar (1990) describe their method of measuring color tuning as follows:[3]

"*Since cortical neurons are often selective for several attributes of a stimulus, and since most cortical neurons respond to achromatic stimuli, our strategy was to characterize the receptive field with achromatic stimuli and then, with stimuli of the favored configuration, vary the chromatic properties for best response*." (Lennie, Krauskopf & Sclar, 1990, p. 651).

Because receptive fields are not likely to be pattern-color separable, the measured color tuning will depend on the selected spatial pattern (e.g., Poirson & Wandell, 1993; 1996). The use of an achromatic stimulus to define the optimal spatiotemporal parameters of a cell may have an influence on which aspect of the color tuning of the cell is reported.

Preliminary reports that promise to provide more complete summaries of the color responsivity have been announced. For example, Cottaris, Elfar & De Valois (1996) have reported measurements of spatio-chromatic color tuning of single-units in area V1. Their measurements are based on a white-noise method that has also been applied to measuring spatio-chromatic tuning in the lateral geniculate nucleus (Reid & Shapley, 1992). Also, Gegenfurtner and his colleagues continue to make measurements in various visual areas (XXX).

Conclusions

The measurements described here and in Engel, Zhang and Wandell (1997) offer us a view of cortical activity that complements the one obtained from single-unit recording. Functional MRI offers a view of the brain that is somewhat analogous to reducing the magnification on our microscope: we see an overview of activity that is much harder to obtain from a

3. Gegenfurtner et al. (1994, see page 458) use a similar method to isolate single units. Both Lennie and Gegenfurtner did perform some additional measurements using non-optimal spatial patterns. These experiments were intended as a check on the generality of their main reported measurements.

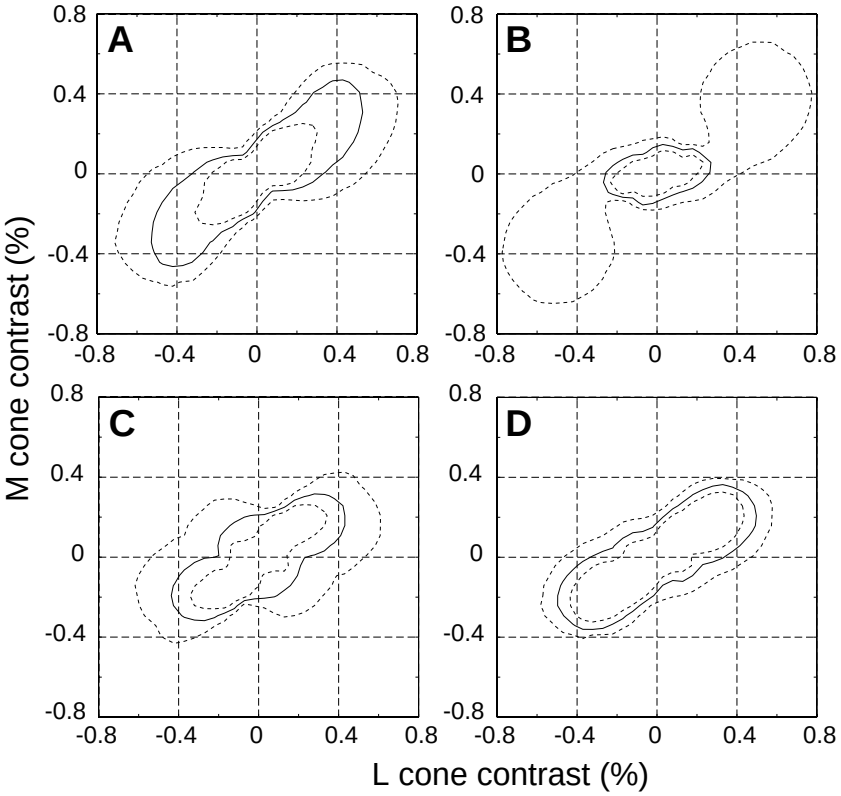

Figure 13.8: Iso-response curves of fMRI signals measured within V1-ROI (panels A and C) and VO-ROI (panels B and D). The axes show the L and M cone ontrast levels of the signal. The smooth contours show the iso-response contour, and the dashed contours show 80 percent confidence intervals around the iso-response contour. Panels (A,B) and (C,D) are for subjects BW and SE, respectively.

sequence of single-unit measurements or even from optical imaging methods. This resolution of measurement offers an opportunity for understanding the cortical architecture of color information processing. At this resolution -- between behavior an single-unit recording, we may be able to learn new lessons about the neural computations that yield our experience of color.

It is too early to have a definitive view of whether cortical computations should be understood in terms of perceptual correlates or basic computational mechanisms. Over the next ten years, we may be able to combine behavioral, single-unit, neuroimaging experiments to clarify whether perception or computation is the organizing principal of the neural representation. By framing and carrying out empirical tests of these hypotheses, we may be able to learn more about the visual computations that determine our visual experience.

Appendix 1: Response amplitude

We describe the method and rationale for estimating the response amplitude by subtracting the estimated noise at the stimulus presentation frequency from the fMRI signal amplitude at that frequency.

Suppose the harmonic response at the stimulus presentation frequency has amplitude r, phase ϕ_r. We represent this quantity as a complex function $r \exp(-i \phi_r)$. Further, we assume that this response is the sum of a signal and noise component,

$$r \exp(-i \phi_r) = s \exp(- i \phi_s) + \bar{n} \exp(-i \bar{\phi}_n),$$

where the amplitude, $\bar{n}$, is a Gaussian with non-zero mean and the phase, $\bar{\phi}_n$, is a uniformly distributed random variable. We measure this response at each voxel.

We compute the expected value, over a group of pixels defining an ROI, of the squared response amplitude as follows:

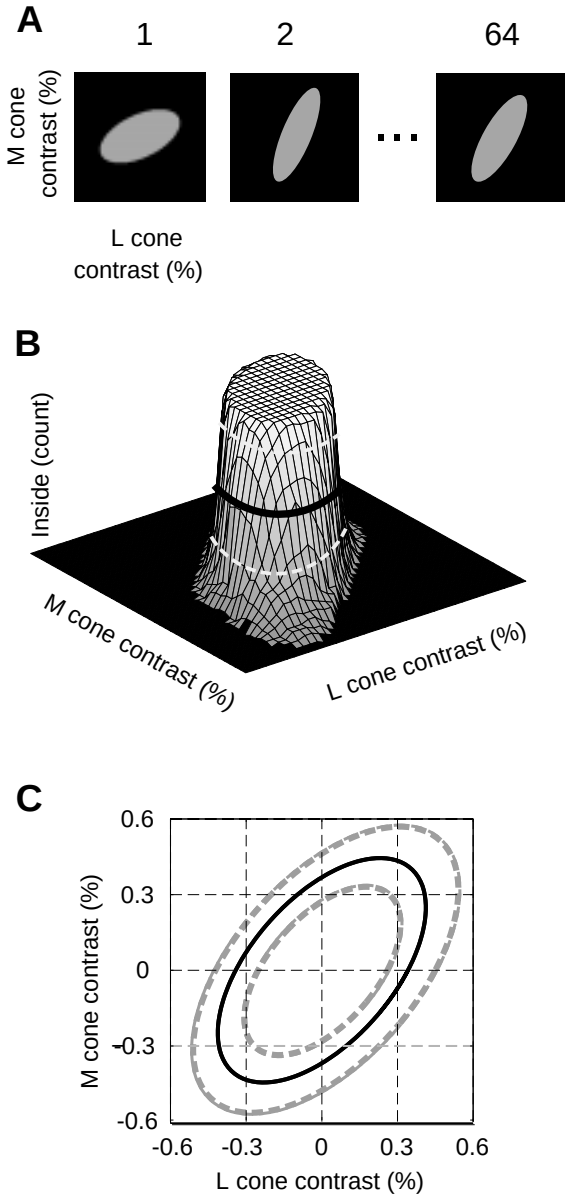

Figure 13.9: A resampling method for determining the iso-reponse contour and confidence intervals. (A) Points on the interior of resampled contours using are shown. (B) A surface plot showing the number of times each stimulus fell inside a simulated contour is shown. The height of the mound shows the number of times each stimulus level falls within the iso-response contour. (C) The solid curve shows the stimulus points that fall inside the resampled contour half the time. The dashed curves show the stimulus points that fall within the resampled contours ninety (outer) and ten (inner) percent of the time.

$$\begin{aligned} \|r \exp(-i\phi_r)\|^2 &= \|s \exp(-i\,\phi_s) + \bar{n} \exp(-i\,\bar{\phi}_n\|^2 \\ &= \|s \exp(-i\,\phi_s\|^2 + \|\bar{n} \exp(-i\,\bar{\phi}_n)\,\|^2 + \\ &\quad 2\|s \exp(-i\,\phi_s)\,\bar{n} \exp(-i\,\phi_n)\,\|^2 \end{aligned}$$

The first and third terms are the squared amplitude of the signal and the noise responses. Because the signal and the noise are uncorrelated, the middle term has an expected value of zero. That is, because the phase term $\bar{\phi}_n$ varies in all directions with equal likelihood, the expectation of the middle term is zero,

$$0 = E\,(\|\,2s\bar{n}\,exp((-i\,(\bar{\phi}_n - \phi_s)))\|^2)$$

$$0 = E(\left\|2s\bar{n}\exp(-i\cdot(\bar{\phi}_n - \phi_s))\right\|^2$$

Hence, the relationship between the squared magnitude of the response, the signal, and the noise is given by the Pythagorean formula

$$E(\|r\|^2) = E(\|s\|^2) + E(\|\bar{n}\|^2).$$

We can estimate the squared magnitude of the signal from (a) the squared magnitude of the response harmonic at the stimulus frequency, and (b) an estimate of the squared magnitude of the noise at the stimulus frequency. Hence,

$$E(\|s\|^2) = E(\|r\|^2) - E(\|\bar{n}\|^2)$$

Finally, notice that $E(\|s\|^2)^{1/2}$ is not equal to $E(\|s\|)$ and that iso-response functions defined by equating with respect to $E(\|s\|^2)$ may be slightly different from those defined by equating with respect to $E(\|s\|)$.

Appendix 2: Resampling

The iso-response contours (solid lines) in Fig. 13.8 represent the set of stimuli that produce a common response amplitude. The iso-response contour and the eighty percent confidence intervals (dashed lines) shown surrounding the contour are computed using a *resampling* procedure. The purpose of this appendix is to explain that procedure.

Each iso-response contour is derived from thirty-six response amplitude measurements. To estimate the variability in this data set, we treat these thirty-six measurements as the entire population and we simulate the effects of repeat experiments by sampling from this population. Specifically, thirty-six random draws (with replacement) are made from the set of thirty-six measurements. A set of random draws is accepted for further analysis only if each color direction is represented by at least one data point. Each measurement represents a response level at a position within the stimulus plane. By gridding the sampled values onto the plane and using a standard two-dimensional contour algorithm (Matlab), we derive a single iso-response contour. This is the *resampled* contour, and we determine those stimulus locations that fall inside and outside the resampled contour.

For the plots in this paper, we performed two hundred resamplings of the data in order to measure the chance that each stimulus point falls inside or outside of a resampled contour. Points near the origin of the stimulus plane, with low contrast in both the L and M coordinates, fall inside the resampled contours nearly every time. Points with high contrast fall outside the contour nearly every time. The iso-response contour (solid line) is drawn though those stimulus levels that fall inside the resampled contour half the time. The confidence interval shown by the outer dashed line shows stimulus points that fall inside a simulated response contour ninety percent of the time. The confidence interval shown by the outer dashed contour show those points that fall within the resampled contour ten percent of the time. Hence, the solid curve represents the typical iso-response contour and the dashed curves define an eighty percent confidence interval about the iso-response contour.

References

Brainard, D. (1989). Calibration of a computer controlled color monitor. Color Researh and Applications, 14, 23-34.

Buxton, R.B. & Frank, L.R. (1997) A model for the coupling between cerebral blood flow and oxygen metabolism during neural stimulation. *Journal Of Cerebral Blood Flow And Metabolism*, 17, 64-72.

Cavanagh, P. & Anstis, S. (1991) The contribution of color to motion in normal and color-deficient observers. *Vision Research*, 31, 2109-2148.

Cottaris, N.P., Elfar, S.D. & De Valois, R.L. (1996) Spatio-temporal luminance and chromatic receptive field profiles of macaque striate cortex simple cells. In *Society For Neuroscience Abstracts*, 22, 951.

Cowey, A. & Heywood, C.A. (1995) There's more to colour than meets the eye. *Behavioural Brain Research*, 71, 89-100.

Dacey, D.M. & Lee, B.B. (1994) The 'blue-on' opponent pathway in primate retina originates from a distinct bistratified ganglion cell type. *Nature*, 367, 731-735.

Dacey, D.M., Lee, B.B., Stafford, D.K., Pokorny, J. & Smith, V.C. (1996) Horizontal cells of the primate retina: Cone specificity without spectral opponency. *Nature*, 271, 656-659.

Engel, S.A., Zhang, X. & Wandell, B.A. (1997) Color tuning in human visual cortex measured using functional magnetic resonance imaging. *Nature*, 388, 68-71.

Fox, P.T. & Raichle, M.E. (1986) Focal physiological uncoupling of cerebral blood flow and oxidative metabolism during somatosensory stimulation in human subjects. *Proceedings of the National Academy of Sciences USA*, 83, 1140-1144.

Fox, P.T., Raichle, M.E., Mintum, M.A. & Dence, C. (1988) Nonoxidative glucose consumption during focal physiologic neural activity. *Science*, 241, 462-464.

Gegenfurtner, K.R., Kiper, D.C., Beusmans, J.M.H., Carandini, M. Zaidi, Q. & Movshon, J.A. (1994) Chromatic properties of neurons in macaque MT. *Visual Neuroscience*, 11, 455-466.

Gulyas, B., Heywood, C.A., Popplewell, D.A., Roland, P.E. & Cowey, A. (1994) Visual form discrimination from color or motion cues: Functional anatomy by positron emission tomography. *Proceedings of the National Academy of Sciences USA*, 91, 9965-9969.

Gulyas, B. & Roland P.E. (1994) Processing and analysis of form, colour and binocular disparity in the human brain: functional anatomy by positron emis-

sion tomography. European Journal of Neuroscience, 6, 1811-28.

Hubel, D.H. & Livingstone, M.S. (1987) Segregation of form, color, and stereopsis in primate area 18. *Journal of Neuroscience*, 7, 3378-3415.

Kleinschmidt, A., Lee, B.B., Requart, M. & Frahm, J. (1996) Functional mapping of color processing by magnetic resonance imaging of responses to selective p-and m-pathway stimulation. *Experimental Brain Research*, 110, 279-288.

Lennie, P., Krauskopf, J. & Sclar, G. (1990) Chromatic mechanisms in striate cortex of macaque. *Journal of Neuroscience*, 10, 649-669.

Lettvin, J.Y., Maturana, H.R., McCulloch, W.S. & Pitts, W.H. (1959) What the frog's eye tells the frog's brain. *Proceedings of the IRE*, 47, 1940-1951.

Lueck, C.J., Zeki, S., Friston, K.J., Deiber, M.-P., Cope, P., Cunningham, V.J., Lammertsma, A.A., Kennard, C. & Frackowiak, R.S.J. (1989) The color center in the cerebral cortex of man. *Nature*, 340, 386-389.

Meadows, J. (1974) Disturbed perception of colours associated with localized cerebral lesions. *Brain*, 97, 615-632.

Poirson, A.B. & Wandell, B.A. (1993) The appearance of colored patterns: pattern-color separability. *Journal of the Optical Society of America A*, 10, 2458-2471.

Poirson, A.B. & Wandell, B.A. (1996) Pattern-color separable pathways predict sensitivity to simple colored patterns. *Vision Research*, 36, 515-526.

Posner, M.I. & Raichle, M.E. (1994) *Images of Mind*. W./ H. Freeman, New York.

Reid, R.C. & Shapley, R.M. (1992) Spatial structure of cone inputs to receptive fields in primate lateral geniculate nucleus. *Nature*, 356, 716-718.

Rodieck, R.W. (1991) Which cells code for color. In *From Pigments to Perception* (eds. Valberg, A. & Lee, B.) pp. 83-93. Plenum Press, New York.

Sakai, K., Watanabe, E., Onodera, Y., Uchida, I., Kato, H., Yamamoto, E., Koizumi, H. & Miyashita, Y. (1995) Functional mapping of the human colour centre with echo-planar magnetic resonance imaging. *Proceedings Of The Royal Society Of London Series B Biological Sciences*, 261, 89-98.

Thulborn, K.R., Waterton, J.C., Matthews, P.M. & Radda, G.K. (1982) Oxygenation dependence of the transferse relation time of water protons in whole blood at high field. *Biochimica et Biophysica Acta*, 714, 265-70.

Wandell, B.A. (1995) *Foundations of Vision*. Sinauer, Ort?.

Zeki, S. (1990) A century of cerebral achromatopsia. *Brain*, 113, 1721-1777.

Zeki, S., Watson, J.D.G., Lueck, C.J., Friston, K.J., Kennard, C. & Frackowiak, R.S.J. (1991) A direct demonstration of functional specialization in human visual cortex. *Journal of Neuroscience*, 11, 641-649.